

## Kinetics of spinodal decomposition in a polymer mixture

N. Kuwahara, H. Sato, and K. Kubota

*Department of Biological and Chemical Engineering, Faculty of Technology, Gunma University, Kiryu, Gunma 376, Japan*

(Received 2 June 1992)

The early-to-late stage of spinodal decomposition in a critical mixture of polystyrene and polymethylphenylsiloxane was studied by time-resolved light scattering over  $1.8 < k < 21.1 \mu\text{m}^{-1}$  and  $0 < t < 502$  h, with  $k$  and  $t$  being the wave number and the elapsed time after temperature quench into the spinodal region, respectively. The time dependences of the maximum intensity of the scattered light  $I_m$  and of the corresponding wave number  $k_m$  were represented by the power laws;  $I_m \propto t^\beta$  and  $k_m \propto t^{-\alpha}$  with  $\alpha=0$  in the early stage,  $\alpha=0.17$  in the intermediate stage, and  $\beta=1.08$  and  $\alpha=0.36$  satisfying  $\beta=3\alpha$  in the late stage. The behavior in the early stage was well expressed by the Cahn-Hilliard theory. These exponent values are almost the same as those observed for Fe-Cr alloys. The behavior of the scaled structure factor in the late stage was expressed by a  $k^{-6}$  dependence in  $k_m < k < 2k_m$  and by a  $k^{-4}$  dependence in  $k > 2k_m$ , in good agreement with the recent theoretical prediction.

PACS number(s): 64.70.-p, 64.90.+b, 82.70.-y

### I. INTRODUCTION

In early works on polymer blends in the vicinity of their critical mixing point, the time evolution of phase separation of polymer blends has been found to behave as well as the other binary liquid mixtures [1-6]. However, recent experiments have shown that polymer blend with low mobility, in which spinodal decomposition proceeds very slowly, behaves like the solid solutions as Fe-Cr alloys [7,8]. In such an experiment the maximum intensity of scattered light,  $I_m$ , increased exponentially with time and the corresponding wave number,  $k_m$ , was independent of time in the early stage supporting the linearized theory of Cahn-Hilliard [9]. It was also found that the time dependence of the wave number at the maximum intensity  $k_m(t)$  was represented by the power laws of  $k_m(t) \propto t^{-\alpha}$ ;  $\alpha=0$  in the early stage,  $\alpha=0.16$  in the intermediate stage, and  $\alpha=0.30$  in the late stage, in good agreement with the result of Fe-40 at. % Cr, contrary to polymer blends of higher critical temperature with high mobility which behave like liquid-liquid mixtures.

Recently it has been predicted that the scattering function in the late stage is not a monotonously unimodal function and is presented by a  $k^{-6}$  dependence in the  $k_m < k < 2k_m$  region and a  $k^{-4}$  dependence (Porod law) in the  $k_m < k$  region [10]. Consequently, a shoulder has been predicted to exist around  $k \sim 2k_m$  in the late stage resulting from the hydrodynamic interaction (mass flow due to the interfacial tension). Such a shoulder was observed in the critical mixtures of isobutyric acid and water [5], 2,5-hexanediol and benzene [5], polydimethylsiloxane and diethyl carbonate [6], and deuterated and protonated 1,4-polybutadiene [3]. On the contrary, only a weak flexion, not a clear shoulder, around  $k \sim 2k_m$  was observed in the scattering function for the critical mixture of polystyrene and polymethylphenylsiloxane, and it was pointed out that the smallness of mobility may result not only in the slow phase separation due to high viscosity but in the different kinetics of phase separation in qual-

ity from the simple binary liquid mixtures [7].

In this paper we report the experimental study of spinodal decomposition in a critical mixture of polystyrene (PS) and polymethylphenylsiloxane (PMPS) having narrow molecular-weight distribution focusing our attention on the behaviors of the phase separating process in the early-to-late stage. The present study enlarges the scattering angle range and observing time range compared with our preceding work to make the detailed analyses of the scattering function possible [7].

### II. EXPERIMENT

Polystyrene ( $M_w = 4 \times 10^3$ ,  $M_w/M_n < 1.02$ , with  $M_w$  and  $M_n$  being the weight- and number-averaged molecular weights, respectively) obtained from Toso Co. Ltd. was used in the present study. The values of density  $d$  and refractive index  $n$  of PS at 25°C were 1.07 g/cm<sup>3</sup> and 1.591, respectively. Polymethylphenylsiloxane obtained from Shin-etsu Chemical Co. was divided into 12 fractions by the solution fractionation in which the solvent was isopropyl alcohol. A fraction characterized as  $M_w = 1.5 \times 10^3$  and  $M_w/M_n < 1.03$  was employed as a sample. The values of  $d$  and  $n$  of PMPS at 25°C were 1.10 g/cm<sup>3</sup> and 1.534, respectively. Therefore, the present system is almost an isorefractive mixture and the effect of multiple scattering is not significant. The PS-PMPS mixtures of 0.35-0.41-wt. % PS in PMPS were dissolved in benzene at a total concentration less than 20 wt. % and each solution was filtered into a regular square quartz cell with an optical path of 2 mm through a Millipore filter of 0.20- $\mu\text{m}$  pore size. The benzene was subsequently allowed to evaporate at 70°C for a week and the polymer blends were further heat treated in a vacuum oven at 90°C for at least 6 months to remove benzene thoroughly, and then the polymer samples were flame sealed under vacuum.

Since the turbidity of polymer blends continues to increase with decreasing temperature over the stable, meta-

stable, and unstable regions, an exact determination of the spinodal temperature  $T_{sp}$  by only the measurement of the transmitted light  $I_t$  at  $\theta=0$  ( $\theta$  being the scattering angle) (cloud point measurement) is difficult. The macroscopic phase separation does not occur in the case of polymer blends. The scattered intensity at  $\theta=90^\circ$  tends to level off as the temperature approaches  $T_{sp}$  [11]. Therefore, the spinodal temperature could be well estimated from the increase and leveling off of the scattered light intensity at  $\theta=90^\circ$ ,  $I_{90}$ , in combination with the decrease of the transmitted light at  $\theta=0$  with decreasing temperature. The temperature dependences of  $I_{90}$  and of  $I_t/I_0$ , with  $I_0$  being the transmitted light intensity at a temperature different from  $T_{sp}$ , for the 38.1-wt. % PS mixture with the optical path of 2 mm are shown in Fig. 1. The temperature of the sample cell was controlled within 1 mK for measurements of  $I_{90}$  and  $I_t/I_0$ . After changing the temperature, the sample was allowed to accomplish a thorough equilibrium for ca. 2 h. Although the phase separation proceeds very slowly, waiting for ca. 2 h is sufficient to check whether the sample is still within the stable region or not. In fact, no noticeable changes of  $I_{90}$  and of  $I_t/I_0$  were detected at the temperature 0.1 °C higher than  $T_{sp}$ . The value of  $T_{sp}=31.9^\circ\text{C}$  could be evaluated from the leveling off as to the increase of  $I_{90}$ . The concentration dependence of the spinodal temperature thus obtained is shown in Fig. 2. The difference between the spinodal temperature and the cloud point temperature is not clear enough because the experimental concentration range is fairly restricted in the present study. Since both of the polymer samples have narrow molecular-weight distributions, the present method is sufficient to determine the critical temperature and the critical concentration. It is estimated that the critical temperature  $T_c=31.9\pm 0.1^\circ\text{C}$  and the critical concentration  $w_c=38.1\pm 0.2$  wt. % PS. Nojima *et al.* used the same polymer blend as the present study though the molecular weights of PS and PMPS are a little larger [2]. In their PS-PMPS mixture  $T_c$  is about  $85^\circ\text{C}$  due to higher molecular weight and  $w_c$  is located fairly far from the top of the spinodal curve, contrary to the present case. This should be caused by the broad molecular-

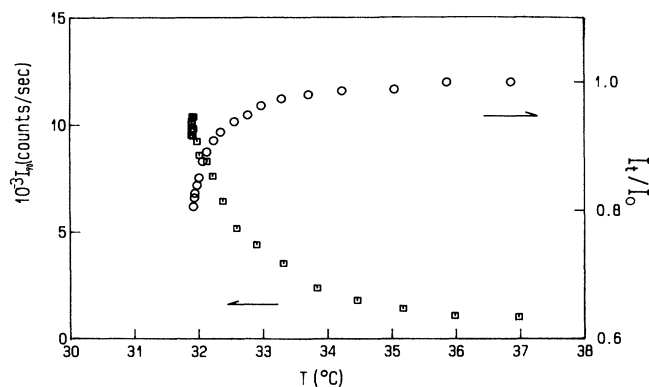


FIG. 1. The temperature dependence of the intensity of scattered light  $I_{90}$  at  $\theta=90^\circ$  ( $\square$ ) and the transmitted light  $I_t$  at  $\theta=0$  ( $\circ$ ).

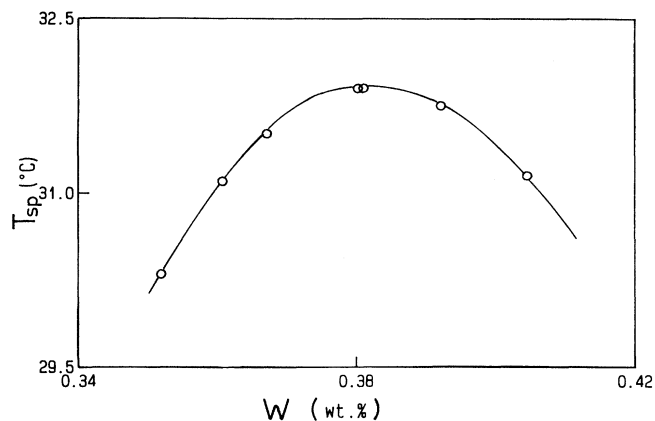


FIG. 2. The concentration dependence of the spinodal temperature of the PS-PMPS mixture.

weight distribution of the sample used by them ( $M_w/M_n=1.57$  for PMPS) contrary to the sharp distribution ( $M_w/M_n < 1.03$  for PMPS) in the present study. The spinodal temperature  $T_{sp}$  and the glass transition temperature  $T_g$  of the present polymer blend appeared in comparable range of temperature, though the  $T_{sp}$  is a little higher than  $T_g$  [2]. The mobility of the polymer mixture is so suppressed in the temperature region under consideration that phase separation should proceed very slowly as compared with other polymer blends studied in the earlier works. The intensity of scattered light changed little, in fact, during a single angular scan of measurement because of low mobility.

The critical PS-PMPS mixture was prepared in a rectangular quartz cell with a short optical path of 0.1 mm according to the procedure of sample preparation mentioned above. The experimental arrangement is shown in Fig. 3. The incident laser beam of wavelength in vacuum  $\lambda_0=632.8$  nm passed through a pinhole ( $P0$ ), a microscope slide ( $G$ ), a convex lens ( $L$ ), a pinhole ( $P3$ ), and the sample ( $S$ ), and it reaches a light trap ( $LT$ ). The intensity of the incident beam was monitored with a microscope slide ( $G$ ), pinhole ( $P1$ ), and photodiode ( $D1$ ) assembly. Scattered light intensities were detected by a pinhole ( $P2$ ) and photodiode ( $D2$ ) assembly mounted on the axis of a rotational table. The intensity of the unscattered beam was also measured by this assembly located at  $\theta=0$  to evaluate the amount of turbidity. The temperature of the silicon oil bath ( $T$ ) for the sample cell was controlled within 5 mK over 3 weeks which was the time span of the longest run. In order to reduce the stray light scattered by silicon oil-glass interfaces, the silicon oil bath made of frosted black ebonite was used. Temperature quench into the spinodal region was achieved by the temperature jump method (temperature decrease) and the quench depth is defined by the difference of temperature from  $T_c$ .

The scattered light intensities were measured for the 28 scattering wave numbers  $k [= (4\pi n/\lambda_0)\sin(\theta/2)]$ , where  $n$  is the refractive index of the medium ( $n=1.556$  for the critical PS-PMPS mixture) and  $\theta$  is the scattering angle, ranging  $1.8\text{--}21.1\ \mu\text{m}^{-1}$  ( $\theta=6.7^\circ\text{--}86.3^\circ$ ). Angular measurements were corrected for constant incident beam,

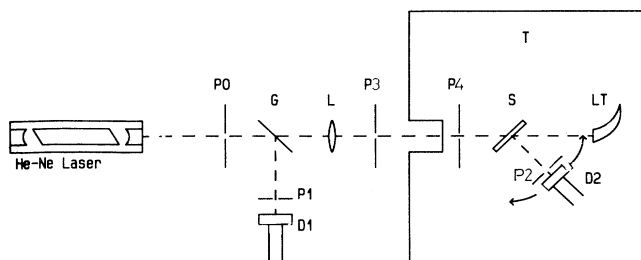


FIG. 3. The schematic diagram of the apparatus.  $P_0$ ,  $P_1$ ,  $P_2$ ,  $P_3$ ,  $P_4$ : pinhole;  $G$ : microscope slide;  $L$ : convex lens;  $D_1$ ,  $D_2$ : photodiode;  $S$ : sample;  $LT$ : light trap;  $T$ : bath.

turbidity, and background. The attenuation corrections for the intensity data were 36% at most. Comparing with our preceding experiment [7], the present system makes the correct determination of the scattering angle and the observation at the widest scattering angle range possible.

### III. RESULTS AND DISCUSSION

A three-dimensional graphic display of the present experimental data is shown in Fig. 4, where the scattered intensity is plotted as a function of  $k$  and of  $t$  for a  $2.0^\circ\text{C}$  temperature quench. The wave number  $k_m$  for the maximum intensity is traced by a dashed curve.  $k_m$  is regarded as the inverse proportion to the average cluster size in the phase separating medium. Curves continue to have a maximum intensity with a constant wave number of  $k_m = 11.4 \mu\text{m}^{-1}$  over an appreciable time range of  $0 < t < 65$  min and the intensity growth is accelerative and almost exponential over the whole  $k$  range. Figure 5 shows the logarithmic plot of the scattered intensity in order to show more clearly the increase of the scattered intensity at early times. The result obtained in the early time region is in fairly good agreement with the prediction of the Cahn-Hilliard linearized theory for spinodal

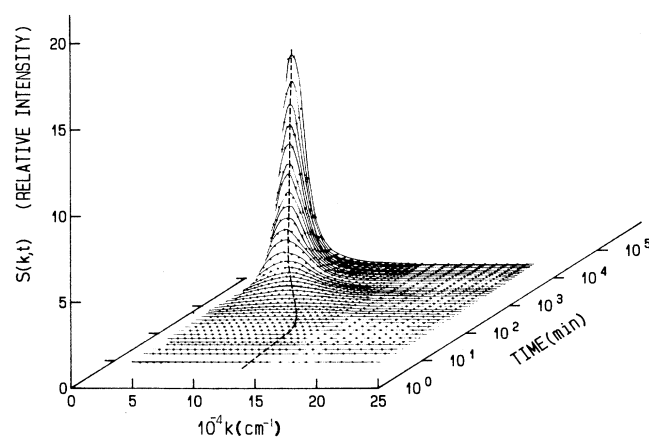


FIG. 4. Three-dimensional graphic display of the scattered intensity as a function of wave vector  $k$  and of time  $t$  after a  $2.0^\circ\text{C}$  quench below the critical temperature  $T_c$ . The locus of the maximum intensity is indicated by a dashed line.

decomposition. It should be noted that the time scale in which spinodal decomposition proceeds is 10–100 times as small as those of other polymer blends observed at higher temperature reported so far [1]. For the time range of  $t > 65$  min the intensity of scattered light grows further and the position of the peak intensity shifts slowly towards smaller  $k$  with an increase of time.

The time evolution of the scattering pattern is characterized by the peak position  $k_m$  and the peak intensity  $I_m$ . The time dependence of wave number  $k_m(t)$  at the maximum intensity can be scaled to dimensionless quantity by the relation

$$Q_m(\tau) = k_m(t)/k_c, \quad (1)$$

$$\tau = t/t_c, \quad (2)$$

where  $k_c$  is the characteristic wave number (the inverse of the relevant length scale in the process of phase separation) and  $t_c$  is the characteristic time that is dependent on quench depth. There were several suggestions to use the inverse of the correlation length in the stable one-phase region as  $k_c$  [4,12]. For the present polymer-polymer mixture the correlation length is on the order of  $0.01 \mu\text{m}$ . The exact temperature dependence, however, is still unknown (whether the Ising model dependence or the molecular-field dependence). On the other hand, there have been reports that the use of  $k_m(0)$  as  $k_c$  gives the reasonable master curve of  $Q_m(\tau)$  vs  $\tau$ , especially

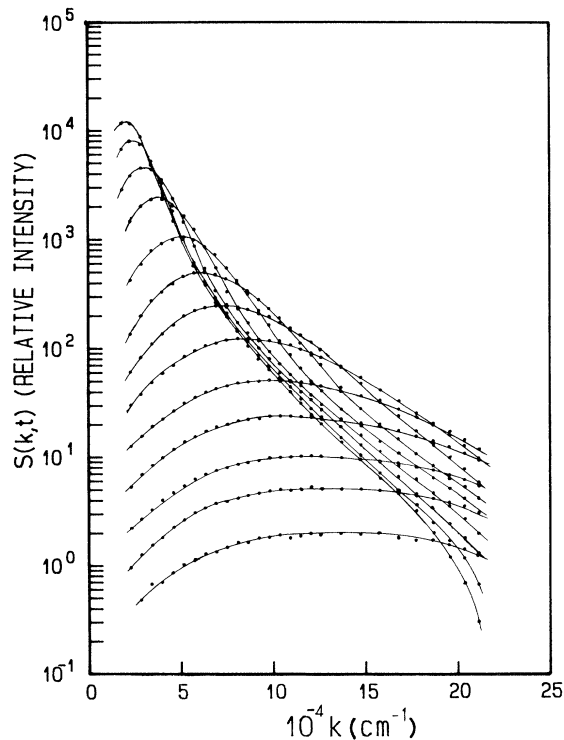


FIG. 5. The logarithmic plot of the scattered intensity as a function of  $k$  at various  $t$  for a  $2.0^\circ\text{C}$  quench. The elapsed time after the quench is 18, 38, 65, 125, 226, 472, 906, 1737, 3516, 7512, 13477, 21875, 30091 min, from the bottom to the top curve, respectively.

when the early stage of spinodal decomposition, where the linearized theory is valid, is observed definitely [1,5-7]. The choice of  $k_c$  and  $t_c$  does not effect the power-law relation of  $Q_m(\tau)$  against  $\tau$ , but its validity can be examined by the superposition for the curves of different quenches.  $t_c$  corresponds to the upper limit of the real time where the unmixing process can be expressed by the linearized theory and it can be evaluated from  $k_m(0)$  and the interdiffusion coefficient  $D^*$  as  $t_c = [D^*k_m(0)^2]^{-1}$ .  $k_m(0)$  and  $D^*$  were determined from the scattered intensity data of Figs. 4 and 5 by use of the so-called  $\frac{1}{3}$ -power plot by Sato and Han [1].  $D^*$  is  $12.0 \times 10^{-13}$  cm<sup>2</sup>/min for a 2.0°C quench. The values of  $k_m(0)$  and  $D^*$  for 1.9 and 3.9°C of the preceding work are  $12.3 \mu\text{m}^{-1}$  and  $12.1 \times 10^{-13}$  cm<sup>2</sup>/min and  $12.2 \mu\text{m}^{-1}$  and  $2.05 \times 10^{-13}$  cm<sup>2</sup>/min, respectively. Contrary to the fact that spinodal decomposition in the liquid-liquid mixture proceeds more rapidly with an increase of the quench depth, spinodal decomposition of the present system does not always proceed more rapidly with an increase of the quench depth due to the strong temperature dependence of mobility. In fact, for the quench depth of 3.9°C the time evolution of phase separation is slower by about 6 times than that for a 2.0°C quench, though the overall features corresponding to Figs. 4 and 5 are quite similar. Moreover,  $k_m(0)$  is almost unchanged at the present quenching temperature range, indicating the temperature dependence of the contribution of interfacial energy according to the linearized theory.

A double logarithmic plot of the scaled wave number  $Q_m(\tau)$  against  $\tau$  is shown in Fig. 6 together with the previous results for 1.9 and 3.9°C quenches. There are no adjusting parameters in this plot. It is first clear that three curves are well superposed to make a universal master curve over about 4 decades of  $\tau$  obtained by the use of  $k_m(0)$  and  $D^*$  mentioned above. It should be noted that Nojima *et al.* [2] and Bates and Wiltzius [3] used the corrected diffusion coefficient for the temperature dependence of mobility by the use of the WLF equation [13] in estimating  $\tau$ . The former obtained relatively good superposition of  $Q_m(\tau)$  vs  $\tau$  but the latter found that the results for several quench depths did not fall onto a universal curve. Second, it is observed that  $Q_m(\tau)$  behaves as simple power laws:

$$Q_m(\tau) \propto \tau^{-\alpha}. \quad (3)$$

Though the entire time evolution is not expressed by a single power law, it can be well expressed by the power laws which are characteristic of three time regions. The experimental results fit well with the power laws with  $\alpha=0$  in the time range  $0 < \tau < 1$  (in the early stage),  $\alpha=0.17$  in  $1 < \tau < 30$  (in the intermediate stage), and  $\alpha=0.36$  in  $30 < \tau$  (in the late stage) in good accordance with the preceding result [7]. The notable characteristics of the present result are that the exponent  $\alpha$  values of 0.17 and 0.36 are very close to the exponent values of  $\frac{1}{6}$  and  $\frac{1}{3}$  for the intermediate and the late stages of spinodal decomposition, respectively, and are quite different from  $\sim \frac{1}{3}$  and  $\sim 1$  observed in the liquid-liquid mixture and polymer blends with higher critical temperature (high

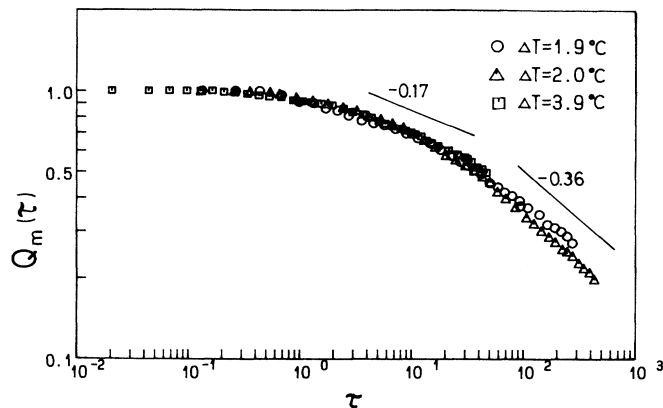


FIG. 6. The scaled time evolution of the scaled wave number at the maximum scattered intensity  $Q_m(\tau)$ . The two inset lines have the slopes of  $-0.17$  and  $-0.36$ . The symbols  $\circ$ ,  $\triangle$ ,  $\square$  stand for the quench depths of 1.9, 2.0, 3.9°C, respectively.

mobility). The time region of  $\alpha=0.17$  spans over more than 1 decade of  $\tau$ . The exponent values of  $\alpha=\frac{1}{6}$  and  $\frac{1}{3}$  and the crossover between them are consistent with the predictions of the Binder-Stauffer theory [14] and the Furukawa theory [15] for the growth of length scale in solids under spinodal decomposition. Numerical simulation by Toral and Marro have also exhibited the crossover of  $\alpha$  from  $\frac{1}{6}$  to  $\frac{1}{3}$  in three dimensions [16]. According to Binder's theory, there are three processes with the different mechanisms of phase separation in spinodal decomposition; the coarsening process obeying the linearized theory, the coagulation process governed by the evaporation of molecules from the cluster surface and their reimpingement resulting in the diffusion of clusters [the exponent value of  $1/(d+3)$  with  $d$  being the dimensionality in Binder's theory], and the condensation process governed by the diffusion of a single molecule one after the other from one stationary cluster to the other (Lifshitz-Slyozov process [17]). The dominant contribution of the movements of molecules in the time evolution of phase separation is in good agreement with the recent theoretical treatment by Puri and Dunweg [18]. By using the cell dynamical system models, Puri and Dunweg have shown that the exponent  $\alpha$  at the late stage appears to be  $\frac{1}{3}$  without hydrodynamic interactions but 1 with hydrodynamics [18]. Because of the very low diffusivity in the present system, the mass flow is suppressed and hydrodynamic interactions could not be effective for the kinetics of phase separation. Therefore, it is plausible that the present system shows behavior similar to that in solid alloys.

On the other hand, Furukawa obtained from the dimensional analyses that the exponent  $\alpha$  is given by  $(d+2+\zeta-h)^{-1}$  [15].  $\zeta$  is a parameter which depends on the contribution of mobility; it is 1 for the surface mobility and 0 for the bulk mobility.  $h$  is a parameter that depends on the contribution to the energy function; it is 0 for the thermal force and 2 for the curvature-driven force. According to this treatment, the combination of  $d=3$ ,  $\zeta=1$ ,  $h=0$  is necessary for  $\alpha=\frac{1}{6}$  and that of  $d=3$ ,

$\zeta=0$ , and  $h=2$  is necessary for  $\alpha=\frac{1}{3}$ . In the intermediate stage, the composition of the clusters does not reach the final coexisting concentration yet, thermal force is the predominant contribution, and the surface tension does not play an essential role yet. On the other hand, the curvature-driven force could be the leading contribution in the late stage where the clusters grow up well and the percolated structure is formed. The reason for the change of the dominant mobility from the surface to the bulk mobility is not clear enough at present. Katano and Iizumi observed that the exponent  $\alpha$  changes from 0.17 to 0.33 for Fe-40 at. % Cr alloy [8]. Therefore, the time evolution of spinodal decomposition in the polymer blends with the low critical temperature like the present case shows entirely different behavior from the simple fluid systems because of their low mobility. On the contrary, in the case of binary liquid mixtures or polymer blends with high diffusivity the Brownian coagulation of clusters (collective mobility) is dominant.

The dynamical scaling concept for spinodal decomposition has shown the time dependence of the maximum intensity of scattering function as

$$I_m(\tau) \propto \tau^\beta. \quad (4)$$

A double logarithmic plot of  $I_m(\tau)$  vs  $\tau$  is shown in Fig. 7 for a 2.0°C quench. As is shown by an inset line,  $I_m(\tau)$  is well described by the power-law relation of Eq. (4) with  $\beta=1.08$  at  $\tau > 10$ . According to the dynamical scaling concept, the inequality  $\beta > 3\alpha$  is held in the intermediate stage and the equality  $\beta=3\alpha$  is held in the late stage. In the present case,  $\beta(1.08) > 3\alpha(3 \times 0.17=0.51)$  in the time range of  $10 < \tau < 30$  and  $\beta(1.08)=3\alpha(3 \times 0.36=1.08)$  in the time range of  $30 < \tau$ . Therefore, the time region of  $\alpha=0.36$  ( $30 < \tau$ ) is indeed the late stage of spinodal decomposition and is not the intermediate stage observed as  $\alpha=\frac{1}{3}$  in binary liquid mixtures. This is shown more evidently in Fig. 8 by plotting  $k_m(\tau)^3 I_m(\tau)$  as a function of  $\tau$ .  $k_m(\tau)^3 I_m(\tau)$  increases gradually with time at  $\tau \lesssim 30$  (in the intermediate stage) and becomes independent of time at  $\tau \gtrsim 30$  (in the late stage). Constancy of  $k_m(\tau)^3 I_m(\tau)$  is consistent with the concept that the scattering function  $S(k, t)$  can be scaled with a single length scale  $R(t)$  in the late stage as

$$S(k, t) \sim R(t)^d F(x), \quad (5)$$

where  $d$  is the dimensionality of the system and  $F(x)$  is a universal scaled structure factor with  $x$  being  $k/k_m(t)$ .  $R(t)$  is considered proportional to  $k_m(t)^{-1}$  in accordance with the result of Fig. 8. The functional form of  $F(x)$  has been proposed by Furukawa as [15]

$$F(x) \sim x^\delta / (\gamma/\delta + x^{\gamma+\delta}). \quad (6)$$

Furukawa gives  $\delta=4$  (thermal fluctuations are not effective, otherwise  $\delta=2$ ) and  $\gamma=6$  ( $2d$  for the critical mixture and the percolation region). The value of  $\gamma=6$  indicates the existence of the self-similar structure characterized by a single length scale in the system.  $F(x)$  is a monotonously unimodal curve and has an  $x^{-6}$  dependence for  $x > 1$ . On the other hand, Ohta and Nozaki

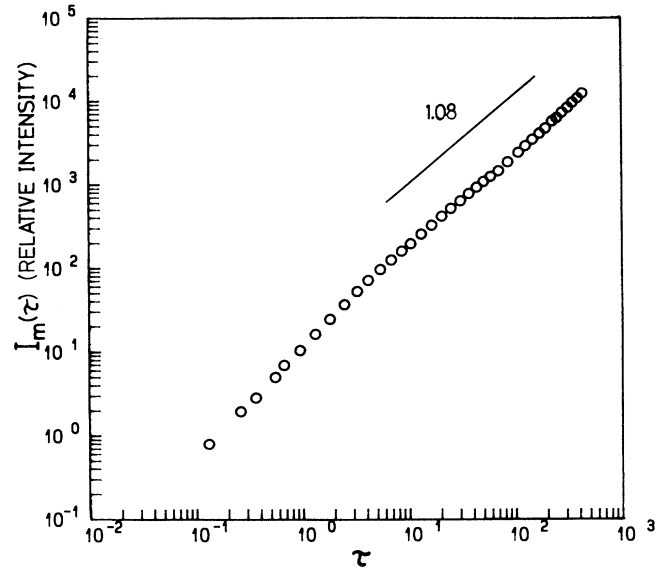


FIG. 7. Double logarithmic plot of the maximum scattered intensity (in relative units) as a function of the scaled time  $\tau$  for a 2.0°C quench. The inset line has a slope of 1.08.

[19] and Koga and Kawasaki [10] have recently proposed theoretically, by taking into account long-range hydrodynamic interactions, that the structure factor is not a unimodal shape but has a shoulder at  $x=2-3$  and the tail of such a shoulder approaches an  $x^{-4}$  dependence (Porod law) with a slight time dependence in the late stage. Such a behavior has been well ascertained for a liquid-liquid mixture [5]. Bates and Wiltzius also observed such a behavior of the structure factor for an isotropic polymer blend [3].

In order to examine the scaled behavior of the scattering function,  $k_m(t)^3 S(k, t)$  are plotted as a function of  $x (=k/k_m)$  in Fig. 9. Figures 9(a), 9(b), and 9(c) correspond to the time region of the intermediate stage, the early-late stage, and the very late stage, respectively. In the intermediate stage, the intensity of  $F(x)$  around its peak gradually increases and each  $F(x)$  does not fall onto a master curve, indicating that the global structure is not

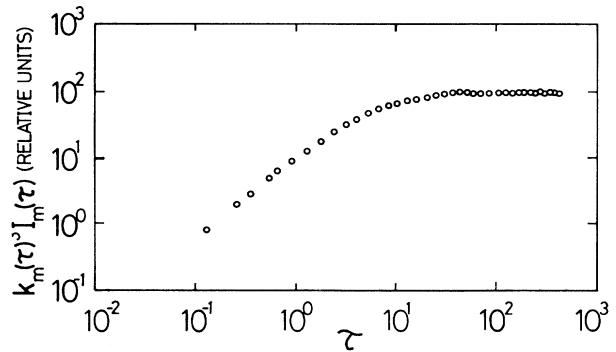


FIG. 8. Double logarithmic plot of  $k_m(\tau)^3 I_m(\tau)$  as a function of the scaled time  $\tau$  for a 2.0°C quench.

scaled yet by a single length scale. However, the tail at  $x > 2$  seems to have an  $x^{-4}$  dependence suggesting that smoothly curved surfaces are developed, though the range of  $x$  is a little restricted. This observation is agree-

able with the results of Katano and Iizumi [8].  $F(x)$  begins to coincide with each other ( $\tau > 30$ ) in the whole range of  $x$  with the increase of  $\tau$  as observed clearly in Figs. 9(b) and 9(c). As  $F(x)$  begins to be superposed, a



FIG. 9. The scaled structure factor plotted as a function of  $k/k_m(\tau) = x$  at various  $\tau$  for a  $2.0^\circ\text{C}$  quench. The symbols denote the scaled time and their meanings are shown in the figure. The two inset lines have the slopes of  $-6$  and  $-4$ . The time region of each figure corresponds to (a) the intermediate to the beginning of the late stage, (b) the early-late stage, and (c) the very late stage.

weak inflection in  $F(x)$  at  $x \sim 2$  appears, indicating that  $F(x)$  has the different power-law relations against  $x$  at each  $x$  region; one ( $x > 2$ ) is the region of  $x^{-4}$  dependence and the other ( $1 < x < 2$ ) is the region of  $x^{-6}$  dependence. The appearance of the  $x^{-6}$  dependence is in accordance with the Furukawa theory suggesting the formation of self-similar structure with entangled surfaces in the phase-separating medium. An  $x^{-6}$  dependence observed for various systems [3,5,6,8,17] implies that the functional form of the scaled structure factor by the Furukawa theory [Eq. (6)] is appropriate for the global structure in the late stage of spinodal decomposition. An  $x^{-4}$  dependence in Figs. 9(b) and 9(c) indicates the formation of a well-developed surface and is in good agreement with the prediction of Ohta and Nozaki [19] and Koga and Kawasaki [10]. The region of  $x$  for such an  $x^{-4}$  dependence is almost the same as that observed by Bates and Wiltzius [3]. On the other hand, though a shoulder at  $x = 2-3$  which has been predicted theoretically [10,19] and observed experimentally in the critical mixtures [3,5,6] is not clearly observed, but only a weak inflection at  $x = 2-3$  is found. This fact seems to be related to the fact that a long-range hydrodynamic interaction might not play an important role in the present system. Recently, Hashimoto, Takenaka, and Jinnai have discussed the late-stage behavior of spinodal decomposition concerning the time dependence of the tail of  $F(x)$  (especially of the shoulder) and divided the late stage into two time regions concerned with the scaling of the local struc-

ture; the development (relaxation) of the surface is faster than that of the global structure [20]. However, such behaviors were not clearly observed in the present PS-PMPS system. This might be related to the fact that the fundamental process of phase separation in the present system could be attributed to the movement of a single molecule, not the mass flow of the cluster as observed in the time dependence of  $Q_m(\tau)$ . Any definite feature about the  $x$  dependence of  $F(x)$  at  $x < 1$  could not be obtained because the scattering angle corresponding to the maximum of scattered intensity was too small.

It may be worthwhile to note that the polymer-polymer mixture shows qualitatively different behaviors concerning phase-separating kinetics, depending on their mobility and temperature range. The smallness of mobility results not only in the slow phase separation due to high viscosity but in the different mechanism of phase separation in quality from the liquid-liquid mixtures. The characterization of such a mechanism should be an important object in processing polymer composites.

#### ACKNOWLEDGMENTS

The authors wish to thank Mr. T. Imai and Miss T. Kubo of Gunma University for their help in the measurements. This work was partly supported by the Grant-in-Aid from the Ministry of Education, Science, and Culture in Japan.

- 
- [1] For example, T. Hashimoto, M. Itakura, and N. Shimidzu, *J. Chem. Phys.* **85**, 6773 (1986); T. Hashimoto, *Phase Transitions* **12**, 47 (1988); T. Sato and C. C. Han, *J. Chem. Phys.* **88**, 2057 (1988).
- [2] S. Nojima, Y. Ohyama, M. Yamaguchi, and T. Nose, *Polymer J.* **14**, 907 (1982).
- [3] F. S. Bates and P. Wiltzius, *J. Chem. Phys.* **91**, 3258 (1989).
- [4] For example, W. I. Goldberg, C.-H. Shaw, J. S. Huang, and M. S. Pilant, *J. Chem. Phys.* **68**, 484 (1978); N.-C. Wong and C. M. Knobler, *ibid.* **69**, 725 (1978); N. Kuwahara, M. Tachikawa, K. Hamano, and Y. Kenmochi, *Phys. Rev. A* **25**, 3449 (1982).
- [5] K. Kubota, N. Kuwahara, H. Eda, and M. Sakazume, *Phys. Rev. A* **45**, R3377 (1992); N. Kuwahara, K. Kubota, M. Sakazume, H. Eda, and K. Takiwaki, *ibid.* **45**, R8324 (1992).
- [6] K. Kubota and N. Kuwahara, *Phys. Rev. Lett.* **68**, 197 (1992); N. Kuwahara and K. Kubota, *Phys. Rev. A* **45**, 7385 (1992).
- [7] N. Kuwahara, H. Sato, and K. Kubota, *J. Chem. Phys.* **97**, 5905 (1992).
- [8] S. Katano and M. Iizumi, *Phys. Rev. Lett.* **52**, 835 (1984).
- [9] J. W. Cahn and J. E. Hillard, *J. Chem. Phys.* **28**, 258 (1958); H. E. Cook, *Acta Metall.* **18**, 297 (1970).
- [10] T. Koga and K. Kawasaki, *Phys. Rev. A* **44**, R817 (1991).
- [11] A. J. Bray and B. M. McCoy, *Phys. Rev. B* **12**, 368 (1975).
- [12] I. M. Lifshitz and V. E. Slyozov, *J. Phys. Chem. Solids* **19**, 35 (1961).
- [13] M. L. Williams, R. E. Landel, and J. D. Ferry, *J. Am. Chem. Soc.* **77**, 3701 (1955).
- [14] K. Binder and D. Stauffer, *Phys. Rev. Lett.* **33**, 1006 (1974).
- [15] H. Furukawa, *Adv. Phys.* **34**, 703 (1985).
- [16] R. Toral and J. Marro, *Phys. Rev. Lett.* **5**, 1424 (1985).
- [17] P. Guenoun, R. Gestaud, P. Ferrot, and D. Beysens, *Phys. Rev. A* **36**, 4876 (1987); D. Beysens, P. Guenoun, and P. Ferrot, *ibid.* **38**, 4173 (1988).
- [18] S. Puri and B. Dunweg, *Phys. Rev. A* **45**, 6977 (1992).
- [19] T. Ohta and H. Nozaki, in *Space-Time Organization in Macromolecular Fluids*, edited by F. Tanaka, M. Doi, and T. Ohta (Springer-Verlag, New York, 1989).
- [20] T. Hashimoto, M. Takenaka, and H. Jinnai, *J. Appl. Crystallogr.* **24**, 457 (1991).